Enstatite aggregates with niningerite, heideite, and oldhamite from the Kaidun carbonaceous chondrite: Relatives of aubrites and EH chondrites?

G. KURAT,[1]* E. ZINNER,[2] F. BRANDSTÄTTER,[1] and A. V. IVANOV[3]

[1]Naturhistorisches Museum, Postfach 417, A-1014 Vienna, Austria
[2]Laboratory for Space Sciences and the Physics Department, Washington University, St. Louis, Missouri 63130, USA
[3]Vernadsky Institute of Geochemistry and Analytical Chemistry, Russian Academy of Sciences, Moscow 117975, Russia
*Corresponding author. E-mail: gero.kurat@univie.ac.at

Abstract–We studied 2 enstatite aggregates (En >99), with sizes of 0.5 and 1.5 mm, embedded in the carbonaceous matrix of Kaidun. They contain sulfide inclusions up to 650 µm in length, which consist mainly of niningerite but contain numerous grains of heideite as well as oldhamite and some secondary phases (complex Fe, Ti, S hydroxides and Ca carbonate). Both niningerite and heideite are enriched in all trace elements relative to the co-existing enstatite except for Be and Sc. The niningerite has the highest Ca content (about 5 wt%) of all niningerites analyzed so far in any meteorite and is the phase richest in trace elements. The REE pattern is fractionated, with the CI-normalized abundance of Lu being higher by 2 orders of magnitude than that of La, and has a strong negative Eu anomaly. Heideite is, on average, poorer in trace elements except for Zr, La, and Li. Its REE pattern is flat at about 0.5 × CI, and it also has a strong negative Eu anomaly. The enstatite is very poor in trace elements. Its Ce content is about 0.01 that of niningerite, but Li, Be, Ti, and Sc have between 0.1 and 1 × CI abundances. The preferential partitioning of typical lithophile elements into sulfides indicates highly O-deficient and S-dominated formation conditions for the aggregates. The minimum temperature of niningerite formation is estimated to be ~850–900 °C. The texture and the chemical characteristics of the phases in the aggregates suggest formation by aggregation and subsequent sintering before incorporation into the Kaidun breccia. The trace element data obtained for heideite, the first on record, show that this mineral, in addition to oldhamite and niningerite, is also a significant carrier of trace elements in enstatite meteorites.

INTRODUCTION

The Kaidun polymict breccia is characterized by an extreme heterogeneity of its components. This carbonaceous chondrite contains, besides a large variety of oxidized and reduced chondritic and achondritic rocks (Ivanov 1989; Clayton et al. 1994; Brandstätter et al. 1996; Zolensky et al. 1996; Zolensky and Ivanov 2003), aggregates consisting mainly of pure enstatite that differ only slightly from each other in texture and minor phases (Kurat et al. 1997; Ivanov et al. 1998). Here, we describe the results of a study of 2 enstatite aggregates with sulfide inclusions and report for the first time the occurrence of heideite in association with niningerite and the trace element abundances of these 2 phases. The aggregates were found in 2 polished sections labeled 01.3.d1 and 01.3.d2 (property of the Vernadsky Institute, Moscow).

EXPERIMENTAL METHODS

The samples were investigated with an optical microscope, analytical scanning electron microscope, electron microprobe, and ion microprobe. Major and minor element contents were determined with an ARL-SEMQ electron microprobe at the Naturhistorisches Museum in Vienna (section 01.3.d1-L) and a Cameca Camebax-microbeam at the Vernadsky Institute (section 01.3.d2-B), both operated at 15 kV accelerating voltage and 15 nA sample current. The samples were analyzed against mineral standards, and ZAF correction procedures were applied. Trace element analyses could only be made in aggregate #d1-L. They were obtained with the CAMECA IMS 3F ion microprobe at Washington University, St. Louis, following the procedures of Zinner and Crozaz (1986). Trace element data were normalized to the Fe contents

of niningerite and heideite and to the Si content of enstatite, respectively, as determined with the electron microprobe.

RESULTS

Texture and Mineralogical Composition of Aggregates

The aggregates consist mainly of enstatite, $MgSiO_3$, the only silicate, have rounded to irregular, angular shapes, and have sizes of 1.5 (d1-L) and 0.5 mm (d2-B), respectively (Fig. 1). They have a granular texture with grain sizes of approximately 100 μm, some pore space, and appear sintered but not well-consolidated. They contain ellipsoidal to irregularly shaped sulfide inclusions, one of which is 650 μm in length (see Fig. 1a). These inclusions are in places tightly intergrown with the granular enstatite matrix. We studied 2 of these inclusions, one from aggregate d1-L, the other from fragment d2-B, in more detail. Both consist mainly of niningerite, (Mg, Fe, Mn)S, but they differ in texture.

Inclusion d1-L-S1 (Fig. 2a) seems to consist of a single crystal of niningerite 650 μm in length. One side of this crystal lies at the boundary of the rock fragment and is in contact with the Kaidun carbonaceous matrix. However, a crack follows a good fraction of the contact (see Fig. 2a). Dispersed throughout the niningerite, with a slight preference for the boundary between aggregate and matrix, are grains of heideite, $(Fe, Cr)_{1+x}(Ti, Fe)_2S_4$, of varying sizes (5–80 μm) and of irregular shapes. They are, in most instances, tightly intergrown with the host, forming lobate interfaces with a few embayments. Some have elongated shapes following the parting plane direction of the host. Small heideites (<10 μm) are more rounded than the large ones. Minor phases present in cracks and open pore space are complex Fe, Ti, S hydroxides (alteration products of heideite), a Mn, Cl-rich fine-grained phase, and some Ca carbonate.

Inclusion d2-B-S1 (Fig. 2b) is polycrystalline and granular. It consists mainly of niningerite grains up to 27 μm in size. An irregularly shaped grain of heideite, about 10×6 μm in size, is located at the periphery of the inclusion. Very small (<2 μm) oldhamite grains are present in the central part. The inclusion was partly destroyed during preparation of the section, which makes it difficult to evaluate its relationship
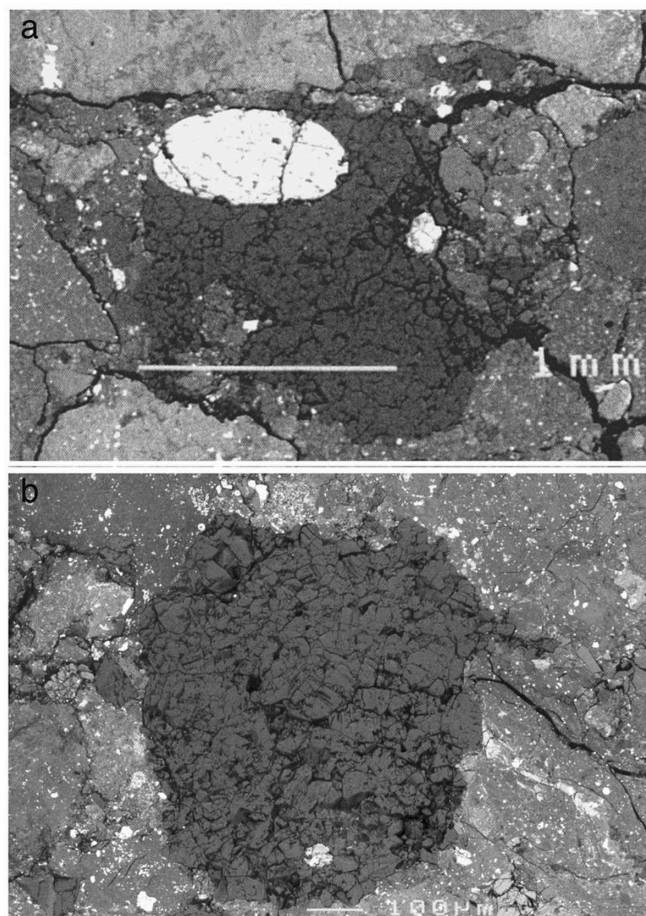

Fig.1. Backscattered electron (BSE) images of the enstatite aggregates d1-L (a) and d2-B (b). Different shades of gray in the enstatite are the result of variations in surface roughness and do not reflect differences in chemical composition.
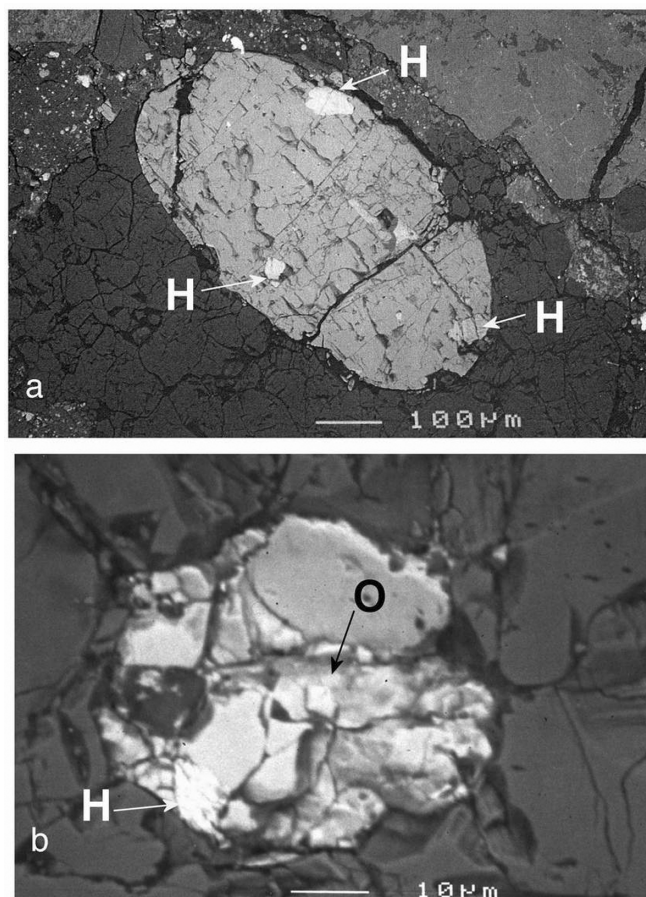

Fig. 2. BSE images of 2 sulfide inclusions: a) inclusion d1-L-S1 consists of niningerite with heideite inclusions (H); b) niningerite inclusion d2-B-S1 has a sizeable heideite inclusion (H) and contains small oldhamite grains (O).

with the surrounding enstatite. However, the interrelationship appears to be complex, as the inclusion does not have a smooth rounded surface but fills grain junctions in the enstatite aggregate and enstatite penetrates the sulfide inclusion in various places. No troilite was found in the inclusions.

Chemical Composition of Minerals

Enstatite, the only silicate encountered, is compositionally quite homogeneous within a given aggregate as well as among the 2 aggregates (Table 1). It is very poor in FeO (mostly 0.1 wt%, in places up to 0.3 wt%) and rich in TiO_2 (up to 0.1 wt%), Al_2O_3 (up to 0.3 wt%), CaO (up to 0.22 wt%), and MnO (up to 0.1 wt%). Niningerites are chemically homogeneous in a given aggregate but differ in composition somewhat between the 2 aggregates (Table 2). They are rich in Ca, Ti, Cr, Mn, and Fe. Their compositions can be approximated by the formulae $(Mg_{0.58}Mn_{0.22}Fe_{0.11}Ca_{0.08})S$ for aggregate d1-L and $(Mg_{0.60}Mn_{0.22}Fe_{0.10}Ca_{0.08})S$ for d2-B.

Also, heideites have homogeneous chemical compositions in a given aggregate and differ between the aggregates (Table 2). The major difference is in the Ni content, which is 0.5 wt% in heideite of aggregate d1-L and 3.2 wt% in that of aggregate d2-B. The compositions of the heideites can be approximated by the formulae $(Fe_{0.99}Cr_{0.42})_{1.41}(Ti_{1.80}Fe_{0.20})_2S_4$ for aggregate d1-L and $(Fe_{0.88}Cr_{0.41})_{1.29}(Ti_{1.85}Fe_{0.15})_2S_4$ for d2-B.

The very small sizes of oldhamite and some other phases did not permit their analysis.

Trace Elements Geochemistry

Niningerite is the phase richest in trace elements (Table 3). The REE pattern (Fig. 3) is fractionated with La(n)

<Lu(n) (chondrite-normalized abundances). The abundances of the heavy rare earth elements (HREEs) vary between 5 × CI (Gd) and 14 × CI (Yb) (for CI abundances, see Anders and Grevesse [1989]). The light rare earth elements (LREEs) are depleted with respect to the HREEs, with abundances of 0.2–4.6 × CI for La to Sm. Europium (Eu/Eu* = 0.12) and Y (Y/Y* = 0.46) have pronounced negative abundance anomalies. Here, Eu* and Y* are the abundances obtained by geometrical interpolation between the neighboring REE of these 2 elements. Niningerite is also rich in Ti, Sc, Cr, Mn, and Li (5 × CI to 90 × CI for Cr and Mn, respectively; Fig. 4). The abundances of Zr, Nb, V, and Na are between 0.9 and 1.5 × CI, and those of Be, B, Sr, Ba, Rb, K, and Co are between 0.02 and 0.4 × CI.

Heideite has, on average, lower trace element contents than niningerite; it has a flat normalized REE pattern at about 0.4–0.7 × CI, except for La, which is slightly depleted with respect to the other REEs (Fig. 3), and it has a negative Eu anomaly. It is rich in Zr (6.5 × CI), Nb (12 × CI), V (9 × CI), Cr (24 × CI), Sr (2 × CI), and B (1.4 × CI); contains Ba, Li, Mn, and Rb at about 1 × CI abundance; Y, Co, K, and Na at abundances between 0.3 × CI and 0.7 × CI (Fig. 4); and is poor in Sc (0.18 × CI) and Be (0.09 × CI).

Enstatite is very poor in trace elements (all <0.13 × CI) except for Sc (1 × CI), Be (0.5 × CI), B (0.86 × CI), and Li (0.19 × CI). The very low contents of Fe (0.0028 × CI), Co (0.0032 × CI), and Sr (0.0022 × CI) and the near-chondritic Fe/Co, V/Cr, and Mn/Cr ratios are remarkable.

DISCUSSION

The 2 studied aggregates show similarities in their texture, mineral modes, and the compositions of their minerals. This fact indicates a similar origin. However, as we could collect trace element data for only one aggregate, the

Table 1. Chemical composition (mean and variations) of enstatite in wt%.[a]

Aggregate	n	SiO_2	TiO_2	Al_2O_3	FeO	MnO	MgO	CaO	Total
d1-L	5	60.4	0.07	0.23	0.20	<0.03	40.3	0.21	101.41
		60.0–61.4	0.03–0.10	0.17–0.30	0.10–0.32	<0.00–0.11	39.8–40.7	0.19–0.22	
d2-B	9	60.4	0.05	0.20	0.14	<0.03	39.4	0.19	100.38
		59.1–61.5	0.03–0.08	0.08–0.30	0.03–0.26	0.00–0.08	38.5–39.9	0.17–0.21	

[a]n = number of analyses. Cr_2O_3, NiO, and Na_2O <0.03 wt%.

Table 2. Chemical composition (mean and variations) of sulfides in wt%.

Mineral	Aggregate	n[a]	S	Fe	Mg	Mn	Ca	Cr	Ti	Ni	Na	Total
Niningerite	d1-L	6	45.5	9.3	20.9	18.2	4.97	1.85	0.30	<0.03	0.28	101.30
			45.3–45.7	9.0–9.7	20.5–21.3	17.6–18.9	4.50–5.20	1.67–2.18	0.21–0.37		0.25–0.32	
	d2-B	7	46.0	8.0	21.3	18.0	4.84	1.49	0.25	<0.03	0.23	100.11
			45.6–47.0	7.2–8.8	20.2–22.9	17.9–18.6	3.40–6.50	1.35–1.62	0.21–0.30		0.17–0.30	
Heideite	d1-L	5	43.0	22.2	<0.33	0.33	0.08	6.9	28.9	0.51	<0.03	101.94
			42.8–43.0	21.3–23.4	0.00–0.13	0.27–0.46	0.05–0.13	6.5–7.3	27.8–29.8	0.30–0.71		
	d2-B	1	40.5	18.1	0.21	0.31	0.08	6.8	28.0	3.20	0.28	97.48

[a]n = number of analyses.

Table 3. Contents of some trace elements in minerals of #d1-L aggregate, ion probe data (error in parenthesis).

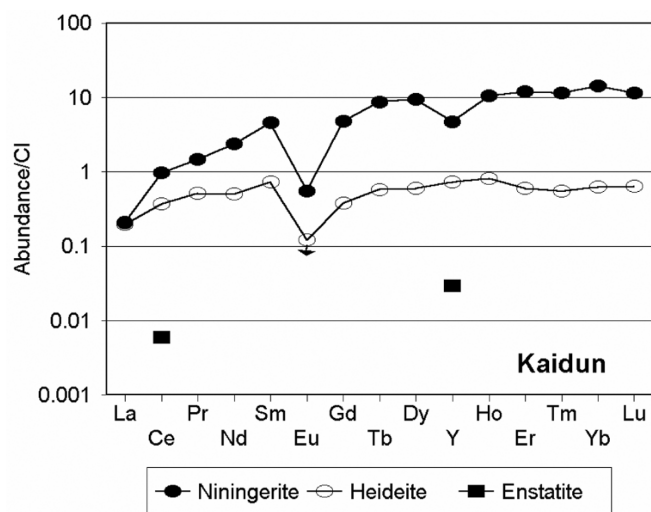| Element	Niningerite		Heideite		Enstatite	
Li	15.5	(2)	1.73	(0.05)	0.31	(0.01)
Be	0.00315	(0.0006)	0.0025	(0.0008)	0.013	(0.001)
B	0.37	(0.03)	1.36	(0.06)	0.84	(0.04)
Na	4288	(4)	2590	(3)	48.8	(0.3)
Al	52.6	(0.3)	14.7	(0.1)	1116.4	(0.9)
P	6.2	(0.5)	19.4	(0.7)	73	(1)
K	13.8	(0.3)	189	(1)	5.3	(0.1)
Sc	43.9	(0.3)	1.02	(0.04)	5.9	(0.1)
Ti	6947	(5)	–	–	466.3	(0.9)
V	70	(0.5)	521	(1)	3.53	(0.09)
Cr	13437	(9)	64390	(17)	184.6	(0.7)
Mn	179800	(37)	2158	(3)	135.3	(0.6)
Fe	93400	(120)	222550	(159)	541	(5)
Co	20.6	(0.6)	176	(1)	1.62	(0.08)
Rb	0.21	(0.02)	2.2	(0.2)	0.045	(0.004)
Sr	3	(0.1)	15	(0.3)	0.0179	(0.0025)
Y	7.3	(0.2)	1.13	(0.06)	0.046	(0.003)
Zr	5.7	(0.2)	24	(0.5)	0.047	(0.006)
Nb	0.3	(0.03)	3	(0.2)	<0.0006	–
Ba	0.08	(0.01)	2.2	(0.2)	0.015	(0.002)
La	0.049	(0.007)	0.047	(0.007)	<0.0006	–
Ce	0.6	(0.04)	0.23	(0.03)	0.0037	(0.0009)
Pr	0.14	(0.01)	0.048	(0.009)	<0.0006	–
Nd	1.09	(0.07)	0.23	(0.02)	–	–
Sm	0.68	(0.09)	0.11	(0.02)	–	–
Eu	0.031	(0.006)	<0.007	–	–	–
Gd	0.94	(0.08)	0.07	(0.02)	–	–
Tb	0.31	(0.02)	0.02	(0.004)	–	–
Dy	2.3	(0.1)	0.15	(0.02)	–	–
Ho	0.57	(0.04)	0.044	(0.008)	–	–
Er	1.9	(0.08)	0.1	(0.01)	–	–
Tm	0.28	(0.04)	0.013	(0.003)	–	–
Yb	2.3	(0.1)	0.1	(0.02)	–	–
Lu	0.28	(0.03)	0.016	(0.004)	–	–

Fig. 3. CI-normalized REE and Y abundances in niningerite, heideite, and enstatite of enstatite aggregate d1-L. The CI abundances are from Anders and Grevesse (1989).
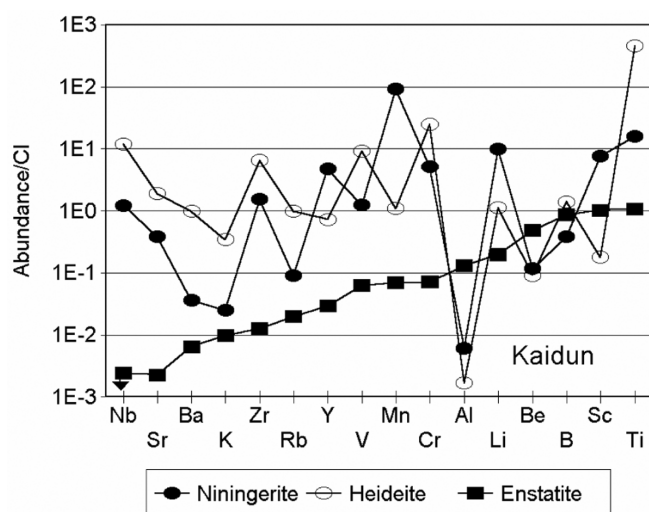

Fig. 4. CI-normalized non-REE trace element abundances in niningerite, heideite, and enstatite of enstatite aggregate d1-L. CI abundances are from Anders and Grevesse (1989).

similar origins of both aggregates can only be inferred from the similar major element contents of their minerals.

Texture and Major and Minor Elements

As described above, enstatite is the only silicate phase of the aggregates. The absence of other silicates, including any melt, indicates that the aggregates as a whole were never melted. The sintered texture of the aggregates supports this view. A chemical characteristic of enstatite is its very low FeO content and low FeO/MnO ratio (~4). Such low values are a signature of reducing conditions and an early condensation formation of the enstatite from or processing in the solar nebula (Klöck et al. 1989).

Niningerite is a typomorphic mineral for EH chondrites (Keil 1968; Ehlers and El Goresy 1988; Lin and El Goresy 2002). Its presence in the Kaidun enstatite aggregates suggests a genetic connection with the EH chondrite population previously described for Kaidun (Ivanov et al. 1986, 1997). On the other hand, the presence of niningerite in the aubrites Shallowater (Keil et al. 1989) and especially Bustee (McCoy 1998), in which heideite was found for the first time, also indicates a relationship between the aggregates and the enstatite achondrites. The equigranular, sintered texture of the aggregates and the lack of any alkali- and aluminum-containing mesostasis favor an aubritic relationship.

The niningerite composition differs drastically from those of niningerites from EH chondrite fragments in Kaidun (Ivanov et al. 1986, 1997) and from other EH chondrites (Keil 1968; Leitch and Smith 1982; Ehlers and El Goresy 1988). The niningerites of the enstatite aggregates have the highest Ca content (~5 wt%, in places up to 6.5 wt%) of all niningerites studied so far (Keil 1968; Rubin and Keil 1983; Ehlers and El Goresy 1988; Lin and El Goresy 2002). They also have high Mn (18 wt%) and low Fe (8–9 wt%; Fe/Mn ~0.5) contents, similar only to those of the "exotic grain" from Qingzhen described by Ehlers and El Goresy (1988). Their rather high Ti content (~0.3 wt%) is noteworthy because such Ti contents were found previously only in Abee niningerite (Rubin and Keil 1983; Ehlers and El Goresy 1988). The Na contents (~0.3 wt%) are similar to those of niningerites in other Kaidun samples.

According to Skinner and Luce (1971), the Ca content of niningerite and alabandite is directly related to the temperature of their formation. The minimum formation temperatures for enstatite chondrites estimated from Ca concentrations in niningerite and alabandite that are in equilibrium with troilite in the solar nebula are 600–800 °C (Skinner and Luce 1971). The absence of troilite in the enstatite aggregates of this study does not allow us to obtain a precise equilibration temperature, but it does allow us to obtain a lower limit of ~850–900 °C. This is the highest equilibration temperature among all meteoritic niningerites known so far.

Heideites have homogeneous chemical compositions in a given aggregate, but differences exist between the aggregates (Table 2). The major difference is in the Ni content, which is 0.5 wt% in aggregate d1-L and 3.2 wt% in aggregate d2-B. Previously, occurrences of heideite have been reported from the Bustee aubrite (Keil and Brett 1974; Kurat et al. 1992; McCoy 1998) and from Kaidun (Ivanov et al. 1995), where it is present as isolated grains and in association with silicates and oldhamite. Heideite from the Kaidun enstatite aggregates is richer in Cr, Mn, and Ni than the previously described samples and coexists with niningerite.

The presence of an oldhamite grain in sulfide inclusion d2-B is of special interest. The problem of oldhamite formation has been discussed thoroughly in recent years from 2 points of view. According to the first, oldhamites in aubrites are primitive condensates (e.g., Kurat 1988; Kurat et al. 1992), or they are the partly metamorphosed relics of a primary nebular condensate (Lodders 1996a). The second point of view connects oldhamite formation in aubrites (Wheelock et al. 1994; McCoy 1998), as well as in unequilibrated enstatite chondrites (Crozaz and Lundberg 1995; Hsu 1998), to crystallization from a sulfide melt, specifically, according to Wheelock et al. (1994), with crystallization during cooling of 2 immiscible sulfide melts (Ca-rich and Mg-, Fe-, Mn-, Cr-rich, respectively). Because oldhamite is an early crystallizing phase and occurs in the trace element-rich niningerite (see below), its origin by crystallization from a sulfide melt seems unlikely.

Mineral inclusions of different hierarchies, i.e., sulfides in silicates and sulfides in sulfides, have rounded to irregular shapes with embayments, which indicates a reaction relationship. This holds for oldhamite and heideite inclusions in niningerite as well as for niningerite inclusions in enstatite. Apparently, these phases were unstable when they were trapped and reacted with a reactant, presumably the ambient gas. The inclusion hierarchy indicates a simple formation sequence: oldhamite and heideite are early phases that were followed by niningerite, which in turn was succeeded by enstatite. Evidence for oldhamite being an early phase is no surprise because this is observed in many cases and is predicted by equilibrium condensation calculations (e.g., Lodders and Fegley 1993). Heideite with its high Fe, Cr, and Ni contents appears not to be an early condensate. However, it could be the reaction product of osbornite, a very refractory and early Ti phase. The reaction between osbornite and the unknown, but presumably gaseous, reactant could have taken place just before or during formation of niningerite. Finally, a small portion of niningerite could have contributed to the formation of enstatite by reaction with an O- and Si-rich vapor. The sulfide phases present in the aggregates probably survived only because they were trapped inside the final reaction product, enstatite.

Trace Elements

The trace element distribution between the phases is quite peculiar. The main phase, enstatite, is poor in most trace elements, poorer than in most enstatite meteorites, similar to but not as depleted as the type III enstatite reported by Hsu and Crozaz (1998). The REEs appear to be fractionated (judging from the concentrations of Y and Ce) with light LREEs being depleted relative to the HREEs (Fig. 3). The enstatite is rich in Sc, Ti, B ($\sim$1 $\times$ CI), Be, and Li (0.5 and 0.2 $\times$ CI, respectively), but only the Al and Be contents are above those of the sulfides (Fig. 4). This indicates a strongly lithophile behavior of Al and Be (the Al and Be contents in sulfides are only $\sim$0.05–0.01 and $\sim$0.2 times that of the enstatite, respectively), which is in stark contrast to the behavior of most of the other trace elements. The elements B, Sc, and Ti have approximately chondritic abundances in enstatite, which is surprising considering the strongly chalcophile behavior of Ti and Sc and the fractionated abundances of all other elements. The moderately volatile elements V, Cr, and Mn are depleted at the 0.06–0.07 $\times$ CI level but are unfractionated relative to each other, similar to the strongly depleted siderophile elements Fe and Co. It is strange that V, Cr, and Mn have the same normalized abundances in enstatite despite the widely different contents in (and partitioning into) sulfides. In Fig. 4, the elements are arranged in order of their abundances in enstatite, and one can clearly see that most lithophile elements behave dominantly chalcophilic. It is also evident from Fig. 4 that the trace element abundances in enstatite and sulfides are independent of each other. The relatively unfractionated abundances of Sc, Ti, and B at $\sim$1 $\times$ CI; V, Cr, and Mn at $\sim$0.07 $\times$ CI; and Fe and Co at $\sim$0.003 $\times$ CI indicate that a primitive chondritic source was involved in the formation of the enstatite. The non-chondritic Fe/Mn ratio in enstatite ($\sim$4 instead of $\sim$100 for CI chondrites), which is comparable to those of Mn-rich silicates in chondrites (e.g., Klöck et al. 1989), also supports a nebular origin and indicates reducing conditions and availability of Mn^{2+} before Fe^{2+} from the nebular gas.

Niningerite is the major carrier of trace elements in our enstatite aggregates. It has a fractionated REE abundance pattern with LREEs <HREEs (Fig. 3), similar to but not as steep as the pattern reported by Crozaz and Lundberg (1995) for niningerite from the ALH A77156 enstatite chondrite and similar to patterns reported for ferromagnesian alabandites from the EL3 chondrite MAC 88136 (Crozaz and Lundberg 1995) and the aubrite Norton County (Wheelock et al. 1994). However, the Kaidun niningerite is clearly richer in REEs than those phases from E chondrites and the Norton County aubrite. It shows a pronounced negative Eu anomaly but no anomalies in the abundances of Sm, Tm, and Yb, indicating that the Eu depletion possibly was caused by crystal-chemical partitioning rather than volatility (e.g., Lodders and Fegley 1993). However, the Eu-rich complementary phase was not found in our thin sections. This phase could possibly be oldhamite, which is present as a very small grain in the sulfide inclusion d2-B-S1. Unfortunately, we have no analytical data for this oldhamite, and we did not find any oldhamite in aggregate d1-L. Niningerite has also a striking Y anomaly, i.e., the CI-normalized abundance is less than half those of Dy and Ho (Fig. 3), a fairly unusual feature. As a Y-rich phase is missing from our assemblage, we do not have a straightforward explanation for this anomaly. Both a crystal-chemical effect and a signature of a vapor depleted in superrefractory elements are possible. Niningerite also seems to have underabundant Zr and Nb ($\sim$1.5 $\times$ CI) but is rich in Sc, Ti, Mn, and Li ($\sim$7–90 $\times$ CI; Fig. 4).

Heideite is much poorer in trace elements than niningerite. In particular, the REEs have abundances at about 0.4–0.7 $\times$ CI, with a flat, unfractionated pattern, except for La, which is somewhat underabundant, and a negative Eu anomaly (Fig. 3). A somewhat similar but LREE-depleted pattern has been reported for caswellsilverite ($NaCrS_2$) from the Peña Blanca Spring aubrite (Fahey et al. 1995). Heideite is very rich in some refractory elements such as Ti, Zr, and Nb but also in V and the moderately volatile elements Cr, Sr, Ba, Li, Rb, K, and Na (Fig. 4).

Most classical lithophile elements apparently prefer the sulfides in our enstatite aggregates. Only Al and Be (and, of course, Si) remain true to their lithophile character. The classical incompatible lithophile elements such as Nb, Zr, REEs, Sr, and alkalis strongly prefer the sulfides with apparent sulfide-silicate partition coefficients of up to >5,000 (Nb)! The preferential partitioning of classical lithophile elements into sulfides indicates highly O-deficient and S-dominated formation conditions for the aggregates. The high lithophile trace element contents in the sulfides are similar to those previously found in enstatite meteorites. They are clearly in disagreement with experimentally determined sulfide/silicate distribution coefficients (Lodders 1996b) but are compatible with sulfide/gas fractionation during condensation under highly reducing conditions (Lodders and Fegley 1993). However, trace element patterns and, in particular, the REE patterns, do not show the signature of vapor fractionation because neither the most refractory nor the most volatile REEs show any anomaly (except for Y, see above). Only Eu is depleted with respect to the other REEs in all phases, an unexplained feature typical of aubrites (Wolf et al. 1983).

Also the pyroxene-compatible transition elements V, Cr, and Mn apparently prefer the sulfides over enstatite. However, as discussed above, these elements have abundances in the enstatite that are obviously independent of the abundances of these elements in the sulfides and, thus, demonstrate that enstatite and sulfides are likely not in chemical equilibrium. That fact suggests the following scenario for the formation of the enstatite aggregates from Kaidun.

Possible Formation Scenario

In an O-deficient environment within the solar nebula, oldhamite (CaS) and osbornite (TiN) precipitated and collected large amounts of trace elements and fractionated REEs with LREE >HREE and a positive Eu anomaly. They were followed by niningerite, (Mg, Mn, Fe)S, that took the remainder of the trace elements still present in the vapor (LREE <HREE and a negative Eu anomaly). During this stage, osbornite became unstable and was converted to heideite. Enstatite precipitation took place under highly reducing conditions and from an environment that had chondritic relative abundances of B, Sc, and Ti as well as V, Mn, and Cr and Fe and Co. During this stage, the previously precipitated sulfides became unstable and reacted with the vapor to contribute to the formation of enstatite. Some sulfides were trapped within the growing enstatite and were, thus, preserved. Three possible scenarios can be envisaged to explain the geochemical characteristics of enstatites: 1) sulfides were formed in a separate place and traveled to the unfractionated enstatite precipitation site where they were collected by the growing enstatite; 2) sulfide precipitation was minor and did not change the general chondritic reservoir, thus allowing precipitation of enstatite at the same location; or 3) enstatite originally acquired trace element abundances according to the sulfide-vapor trace element fractionation but subsequently partly equilibrated with a vapor that had chondritic relative abundances of B, Sc, and Ti, as well as V, Mn, and Cr and Fe and Co. The latter case requires traveling of the enstatite from the sulfide-dominated region to a chondritic one. Because traveling is required for cases (1) and (3), scenario (2) appears to be the most elegant solution. But, the fact that V, Mn, and Cr abundances are not fractionated according to their volatility—as they are in chondrules, chondrites, and the Earth—a vapor-solid re-equilibration event as required by scenarios (1) and (3) appears to be the more likely process.

Classification of Enstatite Aggregates

The trace element distributions reported here are similar to those found in other enstatite meteorites and are in agreement with a classification of the enstatite aggregates as aubrites. In addition, bulk trace element contents estimated from the mineral analyses indicate that the aggregates are trace element-poor rocks with a fractionated REE pattern and a negative Eu anomaly, features that are typical of aubrites (Wolf et al. 1983) but have also been observed in EH chondrites (Crozaz and Lundberg 1995).

CONCLUSION

According to the minerals present, the chemical compositions of these minerals, and their trace element abundance patterns, the 2 enstatite aggregates of this study appear to be related to enstatite achondrites (aubrites), and their mineral chemistry indicates a primitive origin—in accordance with their occurrence as constituents of a primitive, very complex chondritic breccia. These rocks recorded a succession of events that took place in the solar nebula under highly reducing conditions and high sulfur fugacity. Therefore, sulfides such as oldhamite, heideite, and niningerite are most likely pre-enstatite products of condensation. Subsequently, enstatite formed by precipitation from that vapor and, in part, by reaction of that vapor with niningerite. These aggregates traveled to another region of the nebula and incompletely acquired trace elements from a vapor that had chondritic relative abundances of B, Sc, and Ti, as well as V, Mn, and Cr and of Fe and Co. This vapor was reducing, causing Fe and Co to be present mainly in the metallic state (vapor or solid/liquid). Remnants of the early sulfide assemblage survived because they were trapped by the major phase enstatite and, thus, were protected.

The identification of possible aubritic fragments adds another xenolith lithology to the very unusual chondritic breccia Kaidun (see, e.g., Zolensky and Ivanov 2003). Many chondritic and achondritic meteorites contain a wide variety of xenolithic meteoritic matter (e.g., Wilkening 1977), but Kaidun is so far the finest example of an efficient collector of fractionated and unfractionated primitive objects from the solar nebula.

REFERENCES

Anders E. and Grevesse N. 1989. Abundances of the elements: Meteoritic and solar. *Geochimica et Cosmochimica Acta* 53:197–214.

Brandstätter F., Ivanov A. V., and Kurat G. 1996. An ordinary chondrite fragment (R3) in the Kaidun carbonaceous chondrite (abstract). *Meteoritics & Planetary Science* 31:A20.

Clayton R. N., Mayeda T. K., Ivanov A. V., and MacPherson G. J. 1994. Oxygen isotopes in Kaidun (abstract). 25th Lunar and Planetary Science Conference pp. 269–270.

Crozaz G. and Lundberg L. L. 1995. The origin of oldhamite in unequilibrated enstatite chondrites. *Geochimica et Cosmochimica Acta* 59:3817–3831.

Ehlers K. and El Goresy A. 1988. Normal and reverse zoning in niningerite: A novel key parameter to the thermal histories of EH chondrites. *Geochimica et Cosmochimica Acta* 52:877–887.

Fahey A., Huss G., Wasserburg G., and Lodders K. 1995. REE abundances and Cr isotopic composition of oldhamite and associated minerals from the Peña Blanca Spring aubrite

(abstract). 26th Lunar and Planetary Science Conference. pp. 385–386.

Hsu W. 1998. Geochemical and petrographic studies of oldhamite, diopside, and roedderite in enstatite meteorites. *Meteoritics & Planetary Science* 33:291–301.

Hsu W. and Crozaz G. 1998. Mineral chemistry and the origin of enstatite in unequilibrated enstatite chondrites. *Geochimica et Cosmochimica Acta* 62:1993–2004.

Ivanov A. V. 1989. The Kaidun meteorite: Composition and history. *Geochemistry International* 26:84–91.

Ivanov A.V., Skripnic A. Ya., Ul'yanov A. A., Barsukova L. D., Kolesov G. M., and Kononkova N. N. 1986. Chemical composition, mineralogy, and geochemical characteristics of the Kaidun new meteorite. *Meteoritika* 45:3–19. In Russian.

Ivanov A. V., MacPherson G. J., Kononkova N. N., and Stroganov I. A. 1995. Titanium-iron-sulfur-bearing compounds in Kaidun (abstract). *Meteoritics* 30:524.

Ivanov A. V., Migdisova L. F., Zolensky M. E., MacPherson G. J., and Kononkova N. N. 1997. The Kaidun meteorite: An enstatite chondrite fragment with unusual inclusion in the metal. *Geochemistry International* 35:318–328.

Ivanov A. V., Brandstätter F., Kurat G., Migdisova L. F., and Kononkova N. N. 1998. The Kaidun meteorite: An unmelted enstatite aggregate (abstract). *Meteoritics & Planetary Science* 33:A75–A76.

Keil K. 1968. Mineralogical and chemical relationships among enstatite chondrites. *Journal of Geophysical Research* 73:6945–6976.

Keil K. and Brett R. 1974. Heideite, $(Fe, Cr)_{1+x}(Ti, Fe)_2S_4$, a new mineral in the Bustee enstatite achondrite. *American Mineralogist* 59:465–470.

Keil K., Ntaflos Th., Taylor G. J., Brearley A. J., Newsom H. E., and Roming A. D. 1989. The Shallowater aubrite: Evidence for origin by planetesimal impacts. *Geochimica et Cosmochimica Acta* 53:3291–3307.

Klöck W., Thomas K. L., McKay D. S., and Palme H. 1989. Unusual olivine and pyroxene composition in interplanetary dust and unequilibrated ordinary chondrites. *Nature* 339:126–128.

Kurat G. 1988. Primitive meteorites: an attempt towards unification. *Philosophical Transactions of the Royal Society of London Series A* 325:459–482.

Kurat G., Zinner E., and Brandstätter F. 1992. An ion microprobe study of an unique oldhamite-pyroxenite fragment from the Bustee aubrite (abstract). *Meteoritics* 27:246–247.

Kurat G., Zinner E., Brandstätter F., and Ivanov A. 1997. The Kaidun meteorite: An enstatite clast with niningerite and heideite as trace element carriers (abstract). *Meteoritics & Planetary Science* 32: A76–A77.

Leitch C. A. and Smith J. V. 1982. Petrography, mineral chemistry and origin of Type I enstatite chondrites. *Geochimica et Cosmochimica Acta* 46:2083–2097.

Lin Y. and El Goresy A. 2002. A comparative study of opaque phases in Qingzhen (EH3) and MacAlpine Hills 88136 (EL3): Representatives of EH and EL parent bodies. *Meteoritics & Planetary Science* 37:577–599.

Lodders K. 1996a. Oldhamite in enstatite achondrites (aubrites). *Proceedings of the NIPR Symposium on Antarctic Meteorites* 9: 127–142.

Lodders K. 1996b. An experimental and theoretical study of rare-earth-element partitioning between sulfides (FeS, CaS) and silicate and applications to enstatite achondrites. *Meteoritics & Planetary Science* 31:749–766.

Lodders K. and Fegley B. 1993. Lanthanide and actinide chemistry at high C/O ratios in the solar nebula. *Earth and Planetary Science Letters* 117:125–145.

McCoy T. J. 1998. A pyroxene-oldhamite clast in Bustee: Igneous aubritic oldhamite and a mechanism for the Ti enrichment in aubritic troilite. *Antarctic Meteorite Research* 11:32–48.

Rubin A. E. and Keil K. 1983. Mineralogy and petrology of the Abee enstatite chondrite breccia and its dark inclusions. *Earth and Planetary Science Letters* 62:118–131.

Skinner B. J. and Luce F. D. 1971. Solid solutions of the type (Ca, Mg, Mn, Fe)S and their use as geothermometer for the enstatite chondrites. *American Mineralogist* 56:1269–1295.

Wheelock M. M., Keil K., Floss C., Taylor G. J., and Crozaz G. 1994. REE geochemistry of oldhamite-dominated clasts from the Norton County aubrite: Igneous origin of oldhamite. *Geochimica et Cosmochimica Acta* 58:449–458.

Wilkening L. L. 1977. Meteorites in meteorites: Evidence for mixing among the asteroids. In *Comets, asteroids, meteors—Interrelations, evolution and origins,* edited by Delsemme A. H. Toledo: University of Toledo. pp. 389–396.

Wolf R., Ebihara M., Richter G. R., and Anders E. 1983. Aubrites and diogenites—Trace element clues to their origin. *Geochimica et Cosmochimica Acta* 47:2257–2270.

Zinner E. K. and Crozaz G. 1986. A method for the quantitative measurement of rare earth elements in the ion microprobe. *International Journal of Mass Spectrometry and Ion Processes* 69:17–38.

Zolensky M. E., Ivanov A. V., Yang S. V., Mittlefehldt D. W., and Ohsumi K. 1996. The Kaidun meteorite: Mineralogy of an unusual CM lithology. *Meteoritics & Planetary Science* 31:484–493.

Zolensky M. E. and Ivanov A. V. 2003. The Kaidun meteorite: A harvest from the inner and outer asteroid belt. *Chemie der Erde* 63:185–246.